AIAA Guidance, Navigation, and
Control Conference and Exhibit
14-17 August 2000 Denver, CO

A00-37190

AIAA-2000-4549

SIMULATION OF COMBINED ADAPTIVE FEEDFORWARD AND SPATIO-TEMPORAL CONTROL OF AN EARTH OBSERVING TELESCOPE

Kenneth T. Moore, Member 079260, Senior Engineer, SDL, Cincinnati, OH; Stuart J. Shelley, President, SDL, Cincinnati, OH; Thomas D. Sharp, Vice-President, SDL, Cincinnati, OH

Abstract

An active vibration control method incorporating a spatio-temporal filter (STF) and an adaptive feedforward controller is presented as an approach to meet the motion stability requirements for next generation, segmented, optical space systems. In such systems, pointing accuracy must be maintained under conditions that include periodic disturbances such as those induced by the Reaction Wheel Actuators (RWA). When a tachometer signal is available, it can be used in an adaptive feedforward control scheme to cancel the periodic disturbance in the output. A model for the RWA is used that includes harmonics that can excite the flexible modes of the system. The STF controller can be used to increasing damping on these modes, thereby allowing for higher gains and quicker convergence by the feedforward controller. Here, this control method is applied to a state-space model of AFRL's Deployable Optical Telescope (DOT), where the control goal is to maintain the mirror positions while undergoing an RWA disturbance.

Introduction

Many next generation optical space systems such as space based lasers, space observing space telescopes and earth observing space telescopes will utilize very large and/or segmented mirror elements in order to achieve the resolution desired. These systems will require that the elastic deformation of and/or relative motion between elements be reduced to unprecedented levels. The Deployable Optical Telescope (DOT) experiment being developed by the Air Force Research Laboratory (AFRL) requires relative piston motion between mirror segments to be below 10^{-9} meters (10 nanometers). This is roughly the deflection of a street manhole cover under the weight of a dime.

In the context of these position stability requirements, the space environment is not "quiet". Disturbances from reaction wheels, slewing maneuvers and, particularly for space based chemical laser applications, pumps and fluid forces, can cause "large" vibrations.

Active vibration control is a candidate solution for achieving the element stability required, however, classic modern control techniques have disadvantages. Perhaps the most significant of these disadvantages is the need for a complete and accurate model of the plant dynamics. The dynamic response of real-world structural systems is typically very complex. It is difficult to create robust, control oriented models of these systems, particularly if they are time varying which is often the case. To insure control stability and performance these models must include the effects of all dynamics in the frequency range of interest, meaning, typically, many structural vibration modes must be accurately modeled. In many real world applications this modeling effort can represent the majority of the total effort required to develop an active control strategy. Alternative approaches that do not require such an extensive and accurate system model are preferable.

Sheet Dynamics, Ltd., (SDL) is working with AFRL to develop active control concepts that require little knowledge of plant dynamics in order to implement effective, multi-input, multi-output vibration control systems. In addition, the systems will accommodate sensor and actuator failures and can be easily updated to account for changing plant dynamics. These spatio-temporal filtering (STF) algorithms will be demonstrated on the ground based DOT experiment and on the MACE II experiment scheduled to be conducted on the International Space Station in 2000.

Spatio-Temporal Filter based Control

The concept of Spatio-Temporal Filtering is simple; the dynamic response characteristics of a complex, multi-input, multi-output system with many structural modes can be decomposed into its

fundamental components: simple first order systems described by a single pole value and input and output scaling coefficients. These simple, canonical components can easily be controlled or monitored independent of the complexities of the rest of the system.

STF is a sensor/actuator array based approach. It utilizes the sensing and actuation capability of multiple sensors and actuators in an integrated manner rather than individually. It is made feasible by recent developments in lower cost sensors and actuators and associated digital signal processing electronics. It is now feasible to use larger numbers of sensors and actuators for structural vibration control and monitoring.

This approach is unlike classical system identification/model based control. Rather than attempting to identify a complete and accurate model of a complex, possibly time varying system, STF based control attempts to make all of the system response except that associated with the modes of interest completely unobservable. This enables dealing with only the modes contributing to the phenomenon of interest – the rest of the system characteristics are of less concern and are not considered or unnecessarily accounted for; they are intentionally made invisible. This approach allows complex systems that are difficult to accommodate with conventional methods to be controlled and monitored.

Figure 1 illustrates using STF based control for vibration suppression of two critical low frequency modes of a complex system. The figure shows frequency response functions (FRFs) of a physical response, uncontrolled modal coordinates extracted with STF, controlled modal coordinate responses and the resulting closed loop physical system response.

The merit of this basic approach has been recognized by others in the past, however, a practical implementation has not previously been achieved. Meirovitch[2] proposed using strictly spatial or modal filters to implement Independent Modal Space Control (IMSC). The method required a distributed parameter model of the system in order to calculate modal filter coefficients. This is not possible for most systems of practical interest. The STF approach differs in two ways; 1) it filters in both space and time to achieve higher accuracy with fewer sensors and; 2) a practical, reference model based approach is used to adaptively calculate spatio-temporal weighting coefficients. This approach requires minimal knowledge of the system, and given sufficient redundancy, corrects for sensor and actuator failures.

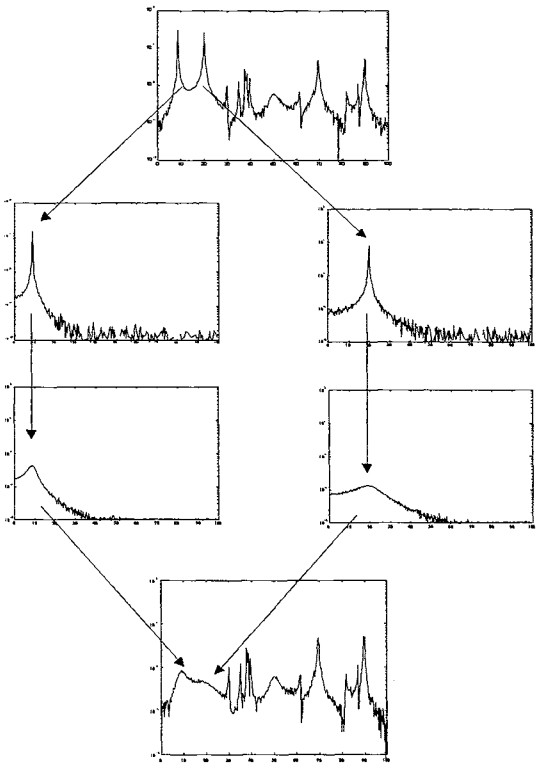

Figure 1. STF Based Structural Vibration Control.

STF Background

STF is an extension of modal, or spatial, filtering which has been investigated by the authors and other researchers for some time[1-3]. Modal filtering utilizes the characteristic that the dynamic response of any real structure is composed of a sum of individual modal responses, each behaving as a single-degree-of-freedom (SDOF) system and each having a particular response shape or eigenvector. The modal filter approach applies sets of scalar, spatial weighting coefficients to responses measured by each element of a sensor array to extract these individual canonical modal responses from the global response of the structure. Note the modal filter is **NOT** related to a conventional bandpass filter. Each channel of the modal filter has output across the entire frequency band, however, it is the output associated with just a single mode.

The basis for modal filtering is the standard modal coordinate transformation that is utilized to simplify the solution, understanding, and analysis of systems

of linear differential equations. For simplicity, consider the undamped, structural case where the common discrete system model consists of a second order linear differential equation with N by N matrix coefficients of mass and stiffness terms.

$$M\ddot{x} + Kx = f \tag{1}$$

Equation 1 may be solved for N linearly independent eigenvectors ϕ_r. Since the eigenvectors are linearly independent the system response, x, may be represented as a linear combination of the eigenvectors weighted by the canonical degrees of freedom or modal coordinates, $\eta_r(t)$.

$$\begin{aligned} x(t) &= \sum_{r=1}^{N} [\phi_r \eta_r(t)] \\ &= \Phi\eta(t) \end{aligned} \tag{2}$$

For the physical case, where control and monitoring is being conducted on a structure, the response vector, $x(t)$, is measured with sensors located at corresponding physical locations and measurement directions. A modal filter is applied to the measured response data, $x(t)$, to extract the modal coordinate response(s), $\eta_i(t)$, of interest. To extract the modal coordinate response for the $i'th$ mode, a vector of spatial weighting coefficients, ψ_i, is sought which has the following characteristics:

$$\begin{aligned} \psi_i^T \phi_r &= 0 \quad i \neq r \\ &= 1 \quad i = r \end{aligned} \tag{3}$$

The inner product between the modal filter vector, ψ_i, and response vector, $x(t)$, is formed which is equivalent to forming a weighted average of the response signals measured at different locations on the structure.

$$\begin{aligned} \psi_i^T x(t) &= \psi_i^T \sum_{r=1}^{N} [\phi_r \eta_r(t)] \\ &= \psi_i^T \phi_i \eta_i(t) \\ &= \eta_i(t) \end{aligned} \tag{4}$$

The resulting scalar quantity is the modal coordinate response, $\eta_i(t)$, for the $i'th$ mode and the vector, ψ_i, is the associated modal filter vector. The above discussion holds for the damped case as well, both proportional and non-proportional[3].

Spatio-Temporal Filtering

The spatio-temporal filter is a generalization of the spatial or modal filter which extends the capabilities by utilizing temporal information; two-dimensional filtering in the space and time dimensions. This reduces the number of sensors required, allows dissimilar sensors to be integrated, and accommodates sensor dynamics.

In order to extract the modal coordinate response of interest with modal filters, the modal vectors, as sampled at the sensor locations, must be linearly independent[3]. This dictates that at least as many sensors as there are independent modes contributing to the measured response are required. Even with modern low cost sensors and DSP electronics, this will be considered a disadvantage in some applications.

The modal filter estimates the modal coordinate response at time k by forming a weighted summation of sensor signals measured at different spatial locations at time k.

$$\hat{\eta}_k = \psi^T x_k \tag{5}$$

An N_i'th order spatio-temporal filter also utilizes N_i past samples of the response information:

$$\hat{\eta}_k = \psi^T \begin{Bmatrix} x_k \\ x_{k-1} \\ \vdots \\ x_{k-Nt} \end{Bmatrix} = \psi^T X_k \tag{6}$$

(2.3)

This introduces a different N_i'th order finite impulse response (FIR) or all-zero filter on each sensor channel. The FIR filters perform different functions depending on the specific implementation; pole-zero cancellation if spatial resolution alone is insufficient to separate modes, accommodating the relative phase between sensors caused by complex (non-proportional damping) modes, selective differentiation if a nonhomogeneous sensor array is used, and correction for some sensor dynamics. Most likely, a combination of the above characteristics will be manifested in the temporal filter component of the STF.

(2.4)

STF Based Control

The STF is not, in itself, a vibration controller. However, design of very effective STF based,

multiple-input, multiple-output, active vibration suppression controllers can entail selection of merely a single scalar control gain parameter for each mode to be controlled.

The reference model utilized to adaptively update the STF coefficients can take the form of a position, velocity or acceleration output model. The adaptive STF will attempt to form a modal coordinate output that matches the reference model. For resonant vibration suppression, a modal coordinate velocity output is often desired to be utilized directly for rate feedback control.

In this case, the control command for each mode consists of:

$$f_c^{(i)} = \hat{\dot{\eta}}^{(i)} \alpha^{(i)} v^{(i)} \tag{7}$$

where $f_c^{(i)}$ is the control command (generally a force command) vector output to control the i'th mode, $\hat{\dot{\eta}}^{(i)}$ is the estimate of the modal coordinate velocity of the i'th mode generated by the STF, $\alpha^{(i)}$ is the control gain and $v^{(i)}$ is the forcing vector. The theoretical control gain required to achieve a certain level of damping can be calculated, however, in practice it is often more effective to manually adjust control gain.

A number of considerations may effect the choice of forcing vector. In general, the forcing vector should be chosen to project strongly on the force appropriation vector (FAV). This is desired since the resulting modal control force is the inner product of the FAV and the control force vector, $l^{(i)^T} f_c^{(i)}$. A good choice of control force vector to maximize this inner product is the FAV vector itself. Since the STF automatically generates the FAV vector it is the logical choice. For each modal controller the control force is:

$$f_c^{(i)} = \hat{\dot{\eta}}^{(i)} \alpha^{(i)} l^{(i)} \tag{8}$$

Control design, then, consists of choosing the control gain, $\alpha^{(i)}$, for each controlled mode. Multiple modal controllers are run in parallel to control multiple modes. In this case, the physical control force command is the sum of the individual modal control forces.

Adaptive Feedforward Control

Adaptive feedforward control is an effective technique for canceling a disturbance for which some measurement of the source is available. It has been successfully used in applications such as acoustic noise cancellation[4] and structural control[5]. In feedforward control, the measured disturbance is fed into the controller to produce the control actuator command signals. This measured disturbance is called the reference signal, and it is usually derived from the primary disturbance (e.g. a tachometer signal from rotating machinery) although a sensor whose output is colored by the plant can also be used. Typically, an adaptive FIR filter is used for the controller because it is more stable than an IIR filter, although lattice forms can be used to keep the adaptation stable. The plant output(s) is used as the error signal to update the coefficients in the FIR filter.

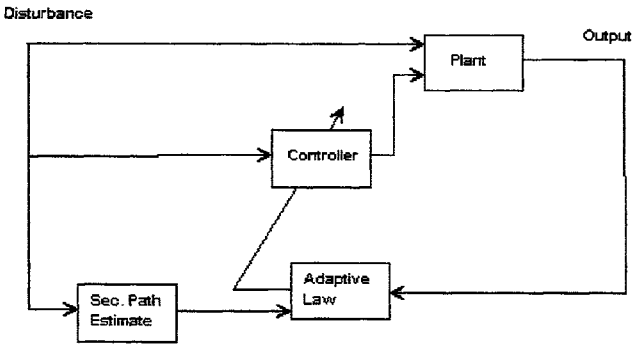

Figure 2 Simple Adaptive Feedforward Control System

A block diagram of a simple adaptive feedforward control system is shown in Figure 2. The method used here is called Filtered-X or Filtered-Reference because the reference signal is filtered by an estimate of the secondary path, or the transfer function between the control input and the sensor (error signal) output. This arises from the use of the LMS algorithm for the adaptation of the coefficients in the controller. Minimization of the expected value of the error signal produces the LMS adaptation law.

$$\tilde{w}(n+1) = \tilde{w}(n) - \mu \hat{x}(n) e(n) \tag{9}$$

Here, w is the vector of weights, and e is error signal from the sensor outputs. The term $\hat{x}$ is the reference signal filtered by the estimate of the secondary path. The parameter μ is the adaptive gain, and is used to adjust the convergence rate of the adaptive law.

Some care must be taken in the choice of the secondary path transfer function. For narrowband disturbance below resonance, Kuo[4] proposes the use of a simple gain for the secondary path, since a difference in phase of up to 90 degrees between the estimated and actual secondary phase does not seem to affect the stability adversely. For SISO adaptive feedforward loops, it is not that critical to model the secondary path gain correctly, since the adaptive gain can be adjusted during design to compensate. When the disturbance is broadband, an FIR (or even an IIR) filter can be used as the secondary path estimate, with the coefficients determined adaptively. This adaptation could occur in parallel with the controller adaptation, or it could occur during a maintenance phase.

Deployable Optical Telescope Model

The objective of the DOT program is to demonstrate autonomous deployment, phase capture, and maintenance of the primary mirrors of an Earth-observing telescope in the presence of realistic operating vibration excitations, including reaction wheel forces, slewing maneuvers and chemical laser disturbances. The AFRL DOT is a functional, ground-based model of a 5-meter diameter sparse array, deployable optical space telescope, as pictured in Figure 3. It has three deployable 60 cm. primary mirrors (1.7 meter array diameter) and a deployable secondary mirror tower. The configuration that is being simulated here does not include the secondary tower because it was still being manufactured at time of publication.

The orientation of each primary mirror is controlled by three piezo-electric stacks mounted on the deployable reaction plate. The optical interferometry provides measurements for the primary mirror axial translation (henceforth called piston) and the primary mirror out of plane rotations (called x and z tilt).

AFRL provided us with a detailed finite-element model of the DOT test structure. This model was solved to determine the first 150 modal frequencies and shapes. Free (unrestrained) boundary conditions were used for the model solution so that the floor attachment nodes would be available as disturbance inputs when the state-space model was formed. A large mass was added to the to simulate floor mounting or attachment to a heavy spacecraft bus; the resulting modal frequencies are then close to those in the fixed case.

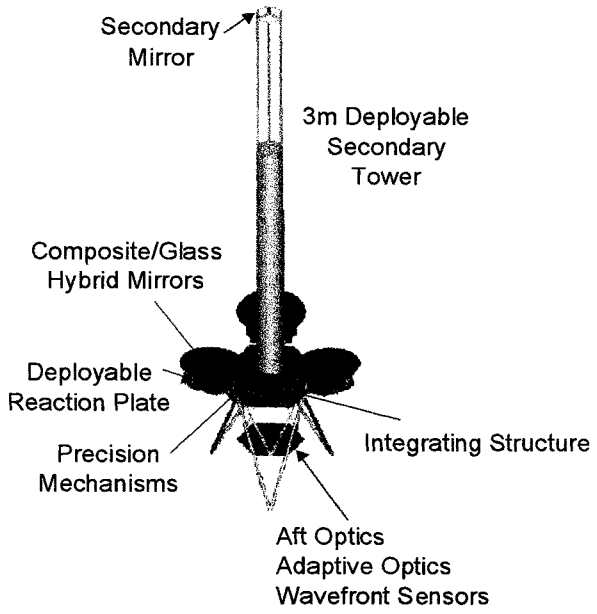

Figure 3 Deployable Optical Telescope Experiment

The mode frequencies and shapes of the DOT were used to assemble a 150-mode state-space model. This large model was initially reduced based on the criteria of observability, controllability, and the piezo-electric DC response. However, for simplicity, the model used here incorporates only the 15 modes with the lowest frequency.

These modes are listed in Table 1.

71.8 Hz	80.8 Hz	121.0 Hz	133.7 Hz	242.6 Hz
73.5 Hz	81.0 Hz	121.6 Hz	135.2 Hz	243.0 Hz
73.6 Hz	82.4 Hz	125.8 Hz	135.3 Hz	249.0 Hz

Table 1 Frequencies of 15-Mode DOT model

These modes are grouped by threes because of the three-fold symmetry of the system. Each group of three modes includes one mode with the mirrors moving in phase, and two modes with out-of-phase motion. Figure 4 shows an FRF from one of the piezoelectric stacks to the Piston output of mirror1.

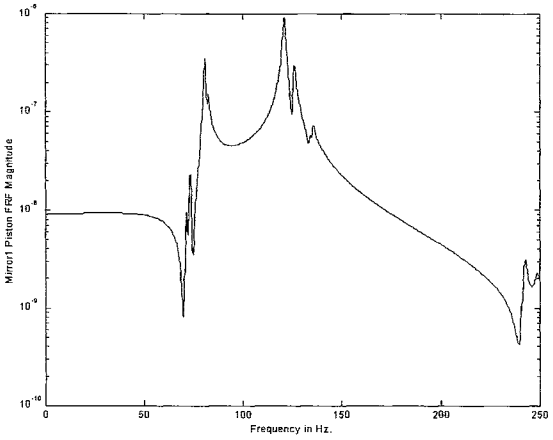

Figure 4 FRF Magnitude of Mirror1 Piezo-stack 1 input to Mirror1 Piston output

The DOT state-space model contains 9 sensor outputs including 1 piston and 2 tilts for each mirror. The nine control inputs representing the piezoelectric stack actuator commands were modeled as force couples between the points on each end of the stack. There are also 6 disturbance inputs representing 3 translational and 3 rotational forces that can be applied to the base of the structure.

DOT Simulation Results

The STF and feedfoward theory presented above is now used to design a control system for the 15-mode DOT model. The control goal is the cancellation in the piston and tilt outputs of a periodic disturbance induced by a spacecraft reaction wheel.

RWA Disturbance

The RWA disturbance model used here comes from an empirical relationship used in Hall[6].

$$\ddot{z} = \left(\frac{2.5e-7}{m_{s/c}} + \frac{6.4e-8}{I_{s/c}} d \right) m_{wheel} \omega_{wheel}^2 \sum_{n=1}^{6} \sin(\omega_n t) \tag{10}$$

Here $\ddot{z}$ is the RWA acceleration disturbance, $m_{s/c}$ and $I_{s/c}$ are the mass and rotational inertia of the spacecraft, d is the appropriate moment arm from the cg to the point of application of the acceleration. m_{wheel} is the reaction wheel mass, ω_{wheel} is the rotation speed, and $\omega_n \in \{[0.35, 1.0, 2.0, 2.8, 5.2, 5.6]\omega_{wheel}\}$ represents the six harmonics of the reaction wheel. For the results presented here, the rotational speed of the reaction wheel was set to 15 Hz. Figure 5 shows the power spectral density of the tachometer signal that includes the fundamental and harmonic frequencies as per the RWA model used here. Changing the reaction wheel speed moves the frequencies of the harmonics higher or lower accordingly. Note that the highest harmonics fall in the range of the structural modes of DOT.

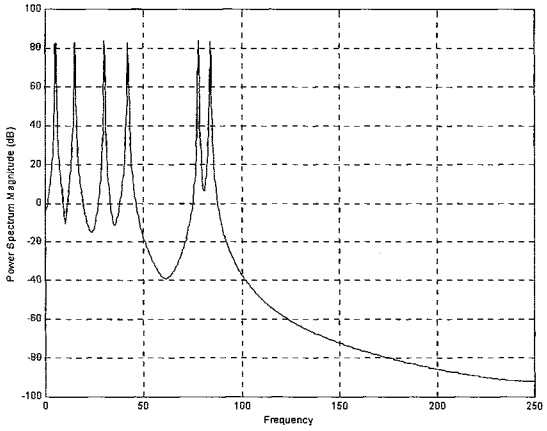

Figure 5 PSD of Tach Reference Signal for 15 Hz RWA rotational velocity.

A detailed examination of the physics of the disturbance caused by RWAs can be found in Masterson[7] and Bialke[8].

To apply this RWA disturbance model to the DOT state-space system, the acceleration in equation 10 is applied to all six base disturbance inputs.

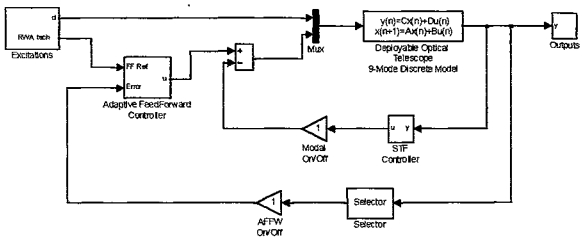

Figure 6 Combined AFFW and STF Simulink model

Control System Design

Figure 6 shows a block diagram of the combined control system that was designed for the DOT model. It includes an adaptive feedforward loop for removing the reaction wheel disturbance, and an

STF loop for suppressing the structural modes of the DOT.

A set of 6 STF controllers were designed to add damping to modes 4 through 9 (see Table 1). These represent the modes that are the most observable in the mirror pistons and tilts. The coefficients were calculated offline using simulation data. The STF usually required 6 or 7 filter taps to produce good isolation of the modes.

The adaptive feedforward controllers were designed as independent SISO loops even though the system is multivariable. A linear combination of the piezo-stack inputs for was determined for each sensor output (piston and tilts for each mirror) using the calculated DC response of the state space model.

$$P = C(-A^{-1})B \tag{11}$$

This gives the combination of actuator inputs that produces a net motion in only the direction of interest.

An FIR filter was chosen with 33 time taps, giving 33 coefficients to be determined adaptively. This number was chosen so that one cycle of the fundamental frequency (15 Hz.) of the reference signal was covered for the system sampling rate of 500 Hz. We experimented with using less time taps with greater time spacing between them, but encountered aliasing problems.

For now, the secondary path was modeled using the true secondary path from the open loop DOT state-space model. This was only done as a preliminary simplification so that the effort could be concentrated on the feedforward adaptation portion of the controller, but there are a couple of important observations to be made. The RWA disturbance has harmonics that can move through the frequency range of the flexible modes, so a high-fidelity model of the controller path is needed. In addition, with an STF modal control loop in the overall control system, the secondary path model is the closed-loop transfer function. If the STF coefficients are obtained adaptively, then the secondary path will also have to be adapted. Soon, we intend to investigate an on-line identification of the closed-STF-loop secondary path transfer function at the frequencies of interest prior to closing the adaptive feedforward loops.

Mirror 1 Piston Adaptive Feedforward Loop

For a first case, one SISO adaptive feedforward loop was closed between the measured and commanded piston for mirror 1. The spatio-temporal filter loop was not closed. This case was simulated with a 500 Hz sampling rate and the adaptive gain was adjusted to attempt to give a reasonably quick convergence without destabilizing the system. Figure 7 shows the resulting time history of the piston of mirror1 for open and closed loop cases. The feedforward controller weights are converging rather slowly, and further increase in the adaptive gain is not possible without destabilizing one of the DOT modes.

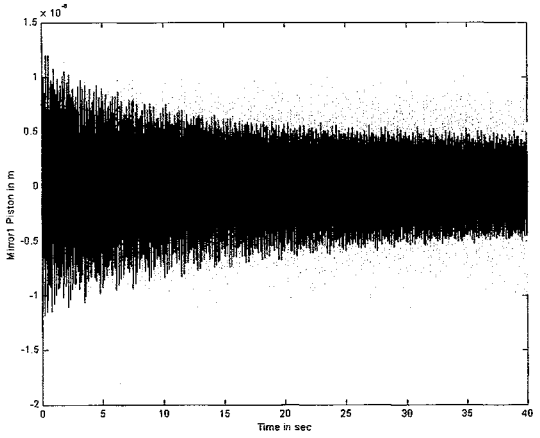

Figure 7 Mirror1 Piston for Piston Loop AFFW with no STF.

When the STF modal controller loop is closed, the adaptive gain of the piston feedforward loop can be increased. The resulting mirror1 piston time history is shown in Figure 8 in comparison with the open-loop piston. Here, the feedforward performance is improved. It is interesting to note that closed-loop piston actually becomes larger than the open-loop piston for a short time, possibly indicating that the STF has moved some zero outside of the unit circle.

With only one sensor output being used in the feedfoward loop, it is quite possible for the other sensor outputs to be worsened by the control system. This is indeed what happens here, as can be seen in Figure 9, where the closed-loop mirror1 x tilt is compared with the open-loop. This signifies that multiple feedforward loops will be required to insure that the disturbance is cancelled in all mirror pistons and tilts. Alternatively, a MIMO single reference method could be used, such as those presented in Kuo[4].

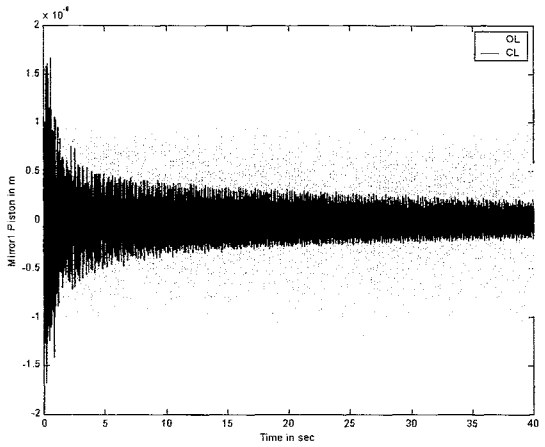

Figure 8 Mirror1 Piston for STF and Piston Loop AFFW. Higher adaptive gain is possible.

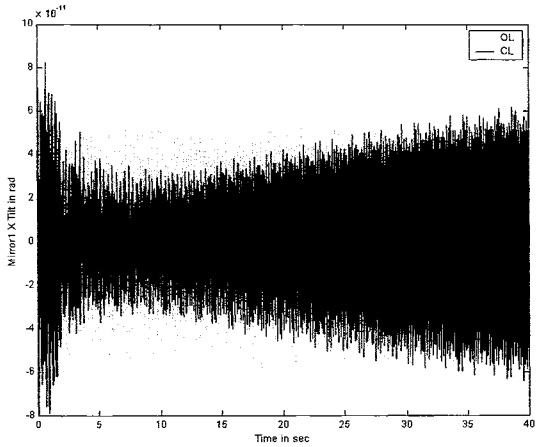

Figure 9 Mirror1 X Tilt for STF and Piston Loop AFFW.

Mirror 1 Tilt Adaptive Feedforward Loop

For the next case, a SISO adaptive feedforward loop was closed between the measured and commanded x tilt for mirror 1. The spatio-temporal filter loop was also closed. Figure 10 shows the closed-loop mirror1 piston compared with that of the open-loop case. As with the piston loop, the adaptive gain was set to provide reasonably quick convergence without destabilizing the system. The tilt loop performance looks good, and it converges quicker that n the piston loop.

Figure 11 shows the power spectral densities of the open and closed loop mirror1 tilts calculated using the last 20 seconds of the time data in Figure 10. Here, it is clear where the harmonics are exciting the flexible modes of the DOT.

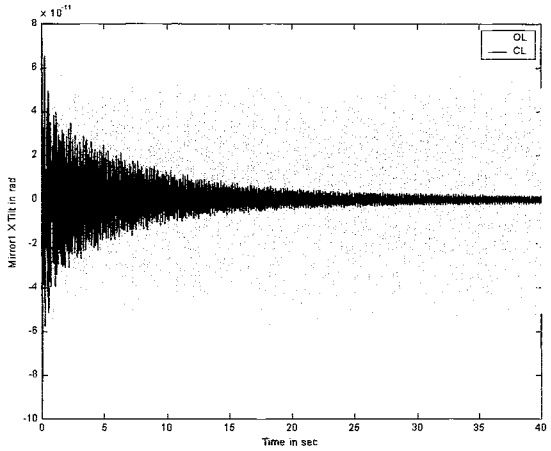

Figure 10 Mirror1 X Tilt for STF and Tilt Loop AFFW.

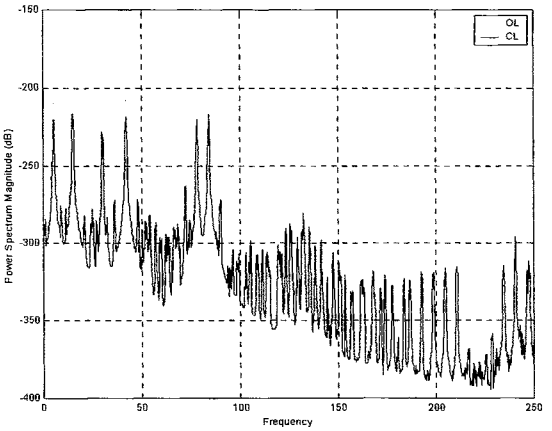

Figure 11 PSD of Mirror1 X Tilt for open and closed loop cases.

Multi-Loop Adaptive Feedforward Control

For a final broadband case, both of the feedforward loops presented above were closed simultaneously. This destabilized the system, and it was necessary to decrease the adaptive gains in both loops. Of course, this slows down the convergence, and the disturbance rejection performance will be worse.

Figure 12 and Figure 13 show the mirror1 piston and x tilt respectively for this 2-loop feedforward case.

It is not currently understood why the adaptive gains chosen when the individual feedforward loops are closed cannot be maintained when they are closed together. In further work, feedforward controllers will be developed using all nine actuators and sensor outputs to determine if that behavior is still exhibited.

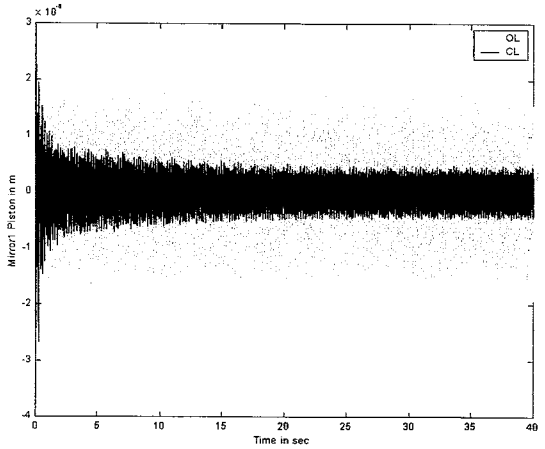

Figure 12 Mirror1 Piston for STF and 2 Loop AFFW.

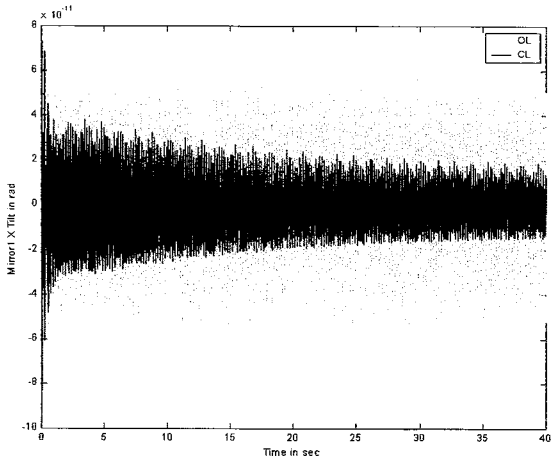

Figure 13 Mirror1X Tilt for STF and 2 Loop AFFW.

Narrowband Adaptive Feedforward Control

When a system is excited by a small number of distinct frequencies, a narrowband adaptive feedforward scheme may be used to simplify the secondary path model. Assuming that these independent signals are available or can be synthesized, a feedforward loop can be designed for each frequency. The secondary path for each loop only needs to include the magnitude and phase for that particular frequency.

The RWA disturbance (Figure 5) contains a fundamental frequency and 5 harmonics, so it is a good candidate for the use of a narrowband method. A block diagram of the narrowband adaptive feedforward controller for mirror piston is shown in Figure 15. Here, there are six loops, where the secondary path magnitude and the adaptive gain have been lumped into a single gain for each loop. A set of adaptive gains was chosen for these 6 adaptive feedforward controllers on the piston variable and for 6 more on the x-axis tilt variable. An STF controller was also designed to add damping to modes 4 through 9. The closed loop system was simulated and compared to open-loop results. Figure 14 and Figure 16 show the closed and open loop time histories of the mirror 1 piston and x tilt respectively for the open and closed loop cases. The narrowband method allows the gain for each excitation frequency to be adjusted independently, so a quicker convergence rate and better overall cancellation of the disturbance is obtained in the output.

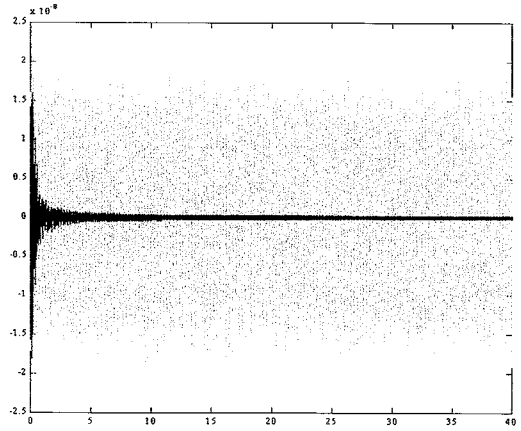

Figure 14 Mirror 1 Piston for Narrowband AFFW with STF.

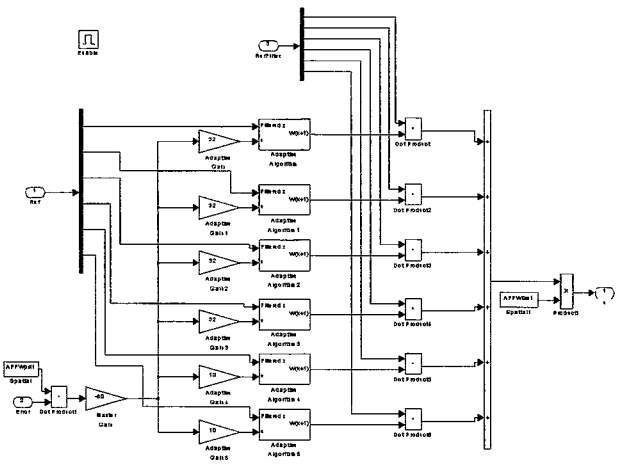

Figure 15 Narrowband AFFW with six frequency loops.

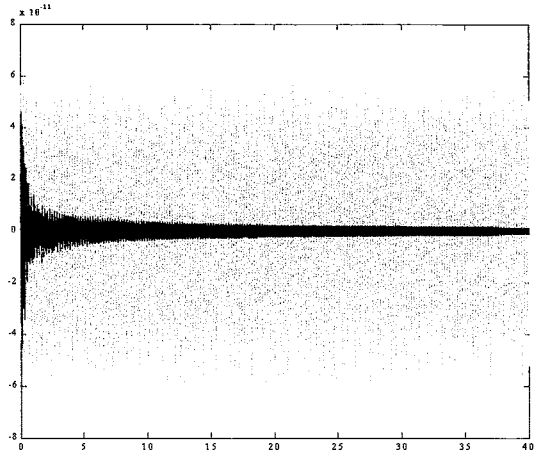

Figure 16 Mirror 1 X Tilt for Narrowband AFFW with STF.

Conclusions

We have proposed a combined adaptive feedforward and spatio-temporal filter design for use in next-generation earth-observing telescopes. This design was implemented in simulation on the 15-mode model of AFRL's Deployable Optical Telescope. Reasonable results were achieved for cancellation of the harmonic disturbance representing excitation by a rotating reaction wheel. The addition of STF to the adaptive feedfoward system was shown to improve the rate of convergence that was obtainable.

There is still much work to be done, as some of the areas that were simplified here (such as the secondary path estimate) will have to be examined. In addition, we will soon have the opportunity to implement our control algorithms on the actual DOT test structure. This will enable us to test our controller design as well as to determine a more accurate model through modal testing.

Acknowledgments

The authors would like to acknowledge the support received for this research under the Phase II SBIR contract awarded by BMDO and managed by the AFRL, Kirtland AFB; Contract F29601-98-C-0159, Adaptive Spatio-Temporal Control: A Practical Approach to Achieve Unprecedented Structural Vibration Control Performance, Robustness, and Reliability, awarded under SBIR Topic BMDO97-012. We would also like to thank Keith Denoyer, Scott Erwin and all those at AFRL, Kirtland who have helped us in this work.

References

1. Shelly, Stuart J., Thomas D. Sharp, and Kenneth T. Moore. "Active Vibration Control of Optical Space Systems." IMAC 1999.
2. Meirovitch, L., Baruh, H. "The Implementation of Modal Filters for Control of Structures." *Journal of Guidance, Control, and Dynamics*, Vol. 8, No. 6, Nov-Dec 1985, pp. 707-716.
3. Shelley, S.J., *Investigation of Discrete Modal Filters for Structural Dynamics Applications*, Department of Mechanical and Industrial Engineering, University of Cincinnati, 1990
4. Kuo, Sen M., and Dennis R. Morgan. *Active Noise Control Systems: Algorithms and DSP Implementations*. John Wiley, New York, 1996.
5. Vipperman J. S., and R. A. Burdisso. "Adaptive Feedforward Control of Non-Minimum Phase Structural Systems." *Journal of Sound and Vibration*, Vol. 183 No. 3, 1995, pp. 369-382.
6. Hall, E. K., and M. W. Vanik. Paper Draft.
7. Masterson, R., and D. Miller. "Development of Empirical and Analytical Reaction Wheel Disturbance Models." AIAA 99-1204, 40th AIAA Structural Dynamics Conference, St. Louis, Mo., 12-15 April 1999.
8. Bialke, Bill. "A Compilation of Reaction Wheel Induced Spacecraft Disturbances." AAS 97-038, 20th AAS Guidance and Control Conference, Breckenridge, CO., Feb. 5-9, 1997.